DNA Photodamage and Repair: Computational Photobiology in Action

Antonio Francés-Monerris, Natacha Gillet, Elise Dumont, Antonio Monari

DNA Photodamages induction and repair: Computational photobiology in action.

Antonio Francés-Monneris,[a,b] Natascha Gillet,[c] Elise Dumont,[c,d] and Antonio Monari[a]

[a]Université de Lorraine and CNRS, LPCT UMR 7019, F-5400 Nancy, France.
[b]Departamento de Química Física, Universitat de València, 46100 Burjassot, Spain
[c]Univ Lyon, ENS de Lyon, CNRS UMR 5182, Université Claude Bernard Lyon 1, Laboratoire de Chimie, F69342, Lyon, France
[d]Institut Universitaire de France, 1 rue Descartes, 75005 Paris

Introduction: DNA Lesions and Their Biological Effects

The fundamental biological role of nucleic acids, and DNA in particular, as the repository of the genetic information, the regulator of its transduction and expression, and the vector of its replication is well established. However, such a role requires that their molecular building blocks should possess a number of crucial properties. In particular, DNA constituents should experience a fairly high stability to avoid the accumulation of chemical modifications, i.e. lesions, which ultimately could lead to mutagenesis and more generally to genomic instability. However, it is wise to moderate such a strong affirmation since, and from a totally reductionist point of view, evolution itself may ultimately be tracked back to genomic mutation.

However, DNA is constantly exposed to an impressive number of stress sources coming both from exogenous and endogenous agents [1–4]. As a most paradigmatic example one may cite reactive oxygen species (ROS),

related to oxidative stress, and produced either by healthy or pathologic metabolic pathways, or by external agents such as drugs or ionizing radiations [1,4–11]. DNA is also constantly exposed to the action of electromagnetic radiation, such as visible or UV light, that may also trigger photophysical or photochemical reactive channels, and hence lead to the accumulation of photoinduced lesions. The latter will, indeed, constitute the main focus of the present Chapter.

In addition, the synergic effects between two or more stress factors can also strongly increase the level of the harmful effects produced to the DNA. Such a synergy will not only enhance the possible occurrence of a given lesion, but may even open totally new chemical pathways, hence leading to the emergence of totally different damages. As a paradigmatic example one can cite the case of DNA photosensitization [12,13], in which a drug absorbing in the infra-red, visible or near UV range, can interact with DNA and subsequently trigger complex photochemical channels, normally involving either energy- or electron-transfer phenomena, ultimately leading to the appearance of DNA photolesions.

To cope with this hostile environment evolution has adopted two strategies: on the one hand the components of nucleic acids have been selected to maximize their photo and chemical stability, hence to minimize the appearance of lesions. On the other hand, efficient DNA repair mechanisms have been developed to reduce the accumulation of DNA damages [14]. In addition, and when the number of lesions overcomes a given threshold, irreversibly compromising the viability of the cell, complex cellular signaling pathways are invoked to trigger apoptosis.

Even if all those strategies are indeed efficient, the accumulation of DNA lesions has been directly related to genomic instability and also to tumorigenesis. In this respect, photolesions are again particularly significant since their accumulation in the skin, mostly due to unprotected sun exposure, has been directly correlated to the apparition and development of malignant tumors such as melanoma [15–19].

However, the induction of DNA lesions is also at the base of widespread therapeutic strategies, particularly for cancer chemotherapy [20–24]. All these approaches are based on the fact that tumor cells generally present a higher number of DNA lesions than healthy ones. Hence, administering drugs that will produce additional DNA lesions will hopefully lead cancer

cells to reach the apoptosis-triggering threshold before the healthy ones. Ideally, this effect should lead to the selective annihilation of the tumor cells and hence the eradication of the disease. As a most paradigmatic example, one of the first, and still widely used, chemotherapeutic agents, cis-platinum [25–27], is indeed relying on this principle and its mechanism of action is based on the formation of covalent bonds with the DNA backbone [28]. However, cis-platinum like most classical chemotherapeutic agents has a very poor selectivity, and hence is plagued by heavy secondary effects, seriously limiting the quality of life of the patients.

Alternative strategies, based on the combined action of drugs and light, are nowadays developed and constitute the domain of photodynamic therapy [29–33] or light-assisted chemotherapy [34–37]. In these protocols a DNA interacting drug, that is non-toxic in the dark, is administered to the patient. Subsequently, light is applied to the area and tissues where the lesion is located to activate the drug via the absorption of electromagnetic radiations and hence trigger the photochemical processes leading to DNA photosensitization [38–42]. Obviously, the selectivity will be dictated by the local application of light that is intended to be restricted only to the area of the cancer lesion. Although attractive, this strategy still suffers from severe drawbacks sometimes limiting its application. Indeed, many different and fundamental problems should be overcome to assure a proper therapeutic efficiency. As a non-exhaustive example we may remind that phototherapy drugs should absorb in the red or infrared portion of the electromagnetic spectrum to assure the coverage of the so-called therapeutic window, and hence the good penetration of light into the biological tissues that is necessary to treat non-superficial lesions [43].

The fascinating complexity underlying the DNA lesions scenario is already apparent from these preliminary considerations. Furthermore, the global picture is also complicated by the fact that the chemical space spanned by the different lesions is extremely large, comprising chemical modifications happening at the DNA backbone or at the level of the nucleic bases [2,6,44,45].

Oxidative DNA lesions may result either in single- or double-strand breaks [46–49] or in the chemical modification of the DNA bases [44,50,51]. Due to the favorable oxidation potential, lesions involving purines, and guanine in particular, are the most common oxidatively generated damages, such

as the widely celebrated 8-oxo-guanine resulting by the action of $^1O_2$. Oxidative pathways may lead to other and more complex outcomes, and in particular to the production of the so called apurinic/apyrimidinic (AP) or abasic sites in which the nucleobase is totally cleaved from the sugar moiety [52–54]. Interestingly, AP sites also represent an intermediate in the DNA repair processes [55]. Oxidatively generated lesions are also commonly produced via DNA photosensitization when the photophysical pathways triggered by the sensitizers lead to the production of $^1O_2$.

Intra-strand base dimerization is the main outcome of DNA photolesions, especially in case of direct UV absorption and as opposed to photosensitization. Because of the more favorable topology and energetic landscape of the involved excited states, pyrimidines, and thymine in particular, will be the most vulnerable nucleobases. As far as thymine photodimers are concerned two main products should be taken into accounts: the so-called cyclobutane pyrimidine dimers (CPD) and the 64-pyrimidinpyrimidone photoproduct (64-PP) [56–60]. While CPD are by far the most commonly produced; 64-PP is characterized by a very high mutagenicity making it extremely dangerous. In addition to dimerization, photo induced inter-strand hydrogen transfer between Watson-Crick bases has also been identified as a pathway leading to DNA photolesions via the formation of nucleobase tautomers [61].

The interaction with external drugs leads also to the production of other less common, yet important, lesions [37,62–64]. Those include the formation of covalently bound, and in some cases bulky, adducts via a chemical coupling to either the backbone or the nucleobases. In some cases, inter-strand cross-links may also be produced, via the formation of a covalent bridge between the 5'- and 3'-strand. Interestingly, inter-strand cross-link may also be produced photochemically by the action of photodissociable drugs [63].

Finally, a particularly intriguing, and highly toxic, class of lesions that are gaining more and more recognition is the one due to DNA protein cross-links, in which an oxidized nucleobase (guanine) forms a covalent bond with aminoacids, such as lysine or asparagine, whose lateral chains present an amine function [44,65]. The same chemical process may also lead to the interaction between DNA and primary amines, such as putrescine, spermine, or spermidine that are widely present in the cellular nuclei [66,67]. Furthermore, if one considers that DNA structure at rest is coiled

around positively charged histone proteins characterized by a high density of lysine and asparagine residues, the relevance of such of lesions cannot be underestimated.

In addition, DNA lesions may be concentrated in a relatively spatial restricted area of the nucleic acids giving rise to the so-called DNA cluster lesions [68–70], i.e. the combination of two or more lesions appearing in between one or two helical turns. As compared to isolated damages, cluster lesions may behave in a correlate way, and hence induce structural deformation of the DNA that can significantly diminish the repair efficiency [71,72].

The actual toxicity varies considerably among the different DNA lesions, and, at first approximation, it depends on the interplay between the frequency of occurrence, the mutagenic potential, and the repair efficiency. Hence, DNA repair enzymes, that should be flexible enough to deal with the very complicated chemical space spanned by the DNA lesions, are one of the key players assuring genome stability in all living organism.

When the DNA lesions involves only one strand, the undamaged complementary one may efficiently serve as a template to guide the repair process and minimize the errors. Two main repair pathways are known: *base excision repair* (BER) [73–77] is active in the case of damages localized on only one nucleobase, while *nucleotide excision repair* (NER) [78–81] is instead used for bulky lesions or intra-strand dimers, such as photolesions. In the case of double-strand breaks or inter-strand cross-links neither NER nor BER are applicable since the complementary strand cannot act as a template. Instead, three different repair mechanism called *non-homologous end-joining*, *microhomology-mediated end joining*, and *homologous recombination* are available [82,83].

One of the key factors to dictate the repair efficiency will be the recognition of the damaged strand by repair enzymes, hence the structural modification induced by the different lesions on the canonical DNA conformations will be crucial to rationalize these processes [71,84]. The organization of nuclear DNA, especially in the case of eukaryotes, is quite complex due to the super-coiling of the nucleic acid in the chromatin structure [85,86]. This organization leads to important consequences for repair, indeed regions of high or low compaction may be characterized by

different repair rates, while the chromatin organization may change in the course of the cellular cycles, and is also related to epigenetic signaling.

Even through this brief and non-exhaustive introduction, it appears that the world of DNA lesions and photolesions, is fascinating yet extremely complex. To achieve a proper rationalization of all the different intertwined relevant phenomena a proper multi-scale approach is needed, that should be able to take into account all the different effects at molecular and systemic level. In particular, molecular modeling and simulation are fundamental to provide an atomistic and electronic resolution of the different phenomena into play, and hence discriminate between different processes and their causes, while predicting or rationalizing complex outcomes.

The computational study of the properties of isolated or hydrogen bonded nucleobases, used as model systems of the extended DNA strands, have been and are still actively pursued. As an example we may cite the study, performed using energy decomposition analysis tools, of the role of cooperativity in hydrogen bonds in the case of canonical and non-canonical structures such as guanine-quadruplexes [87–90].

In addition, the study of isolated systems performed at a high quantum chemical level has also allowed for a constant development and improvement of force fields for molecular dynamics simulations, whose quality is nowadays well established and allows for a proper simulation of the most relevant structural parameters of DNA in different environments [91–94]. Most importantly, such a development has also allowed a good representation of the complex interactions taking place between nucleic acids and proteins, either for compaction, replication, or repair [95–97].

The study of isolated model systems has strongly contributed to understand the molecular bases behind DNA (photo-)lesion appearance and evolution. However, the crude approximations underlying this approach have shown their limitations, once again both from an experimental and theoretical point of view [50]. Indeed, environment dependent distributions of reaction products between solvated nucleotides and oligomeric DNA have been observed, pointing to the fundamental role of the molecular environment in tuning the overall process, both for oxidative and photoinduced DNA lesions. The development of efficient multiscale methods, in particular at hybrid

quantum mechanical/molecular mechanical (QM/MM) level has allowed to rationalize such occurrence with an electronic scale resolution.

The use of QM/MM algorithms has also allowed achieving some clear insights into DNA repair mechanisms, in particular obtaining highly precise and statistically converged free energy profile for the enzymatic reactions, also including photoactivated mechanisms in the case of bacterial systems [98–102]. However, less systematic studies are devoted to the global structural deformations induced by the different classes of lesions on the DNA and their consequence on the repair efficiency, as well as to the coupling between cluster lesions and their effects on the recognition by the repair machinery. To answer such questions an efficient and effective sampling of the conformational space of DNA strands, both solvated and in interaction with repair enzymes, should be performed [71,84]. In other words, it is necessary to enlarge the focus from the purely electronic effects to structural and dynamic perturbations.

In the following sections of this chapter we will provide some example dealing with the study of DNA photolesions production, either by direct light absorption or through photosensitization, and with the related DNA repair mechanisms. We will show that proper multiscale protocols are nowadays available, and that by carefully chosing the right level of theory the description of the entirety of the complex mechanisms into play is available. In particular, we will demonstrate that the journey starting from the description of light/matter interaction, proceeding through the study of photochemical evolutions, and achieving with the elucidation of the biological outcome, has become accessible.

Hence, and in addition to the relevant interest of DNA lesions *per se*, this chapter will also constitute an example illustrating the maturity of molecular modeling and simulation, that is nowadays completely assuming its role as a real computational microscope. Such a maturity has, in our opinion, paved the way to the emergence and the development of a novel, and complementary, scientific approach, computational molecular photobiology, that should be properly recognized. Computational photobiology has been realized by the enormous efforts of a large number of researchers, by the impressive methodological development of the last decades, and also by the change of paradigm switching the focus of molecular modeling and simulation to the multiscale description of the interplay between complex phenomena and complex environments. This

chapter will provide illustrative examples of computational photobiology into actions, clearly highlighting all the novel and fascinating possibilities it can offer to the scientific community.

DNA Photolesions by Direct UV Light Absorption

CPD vs 64-PP (Roberto and Dimitra etc…….) → Toni

Hydrogen Transfer Tautomerization (Valencia, plus Chem. Sciences) → Toni

Photoinduced electron transfer in DNA → Natascha

Modeling DNA Photosensitization

Classical Photosensitization the paradigmatic case of benzophenone

The number of potential DNA photosensitizers is extremely large and it includes drugs, pollutants, and their metabolites. In addition, the great majority of phototherapeutic drugs may be considered as photosensitizers ultimately producing $^1O_2$, upon light absorption and intersystem crossing via the "Type II" photosensitization. Transition metal complexes, especially based on heavy metals such as Ru, Re, and Ir, are also known to induce photosensitization and in some instances have also been proposed for clinical trials [35,36]. Globally speaking the mechanisms inducing photosensitization are different, and comprise energy- and electron-transfer phenomena as well as other more complex photoreactive pathways including H-abstraction from DNA constituents.

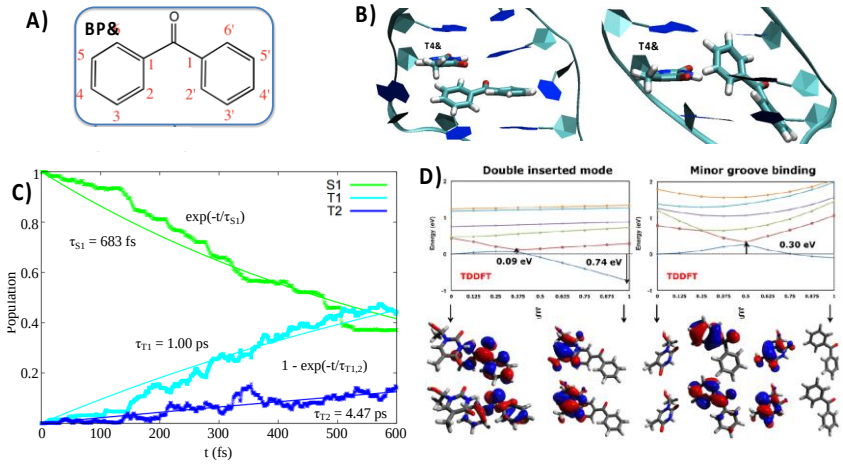

Figure XXX) A) Molecular structure of benzophenone and B) the double insertion (left) and minor groove binding (right) interaction modes with double stranded DNA as obtained from classical MD. C) Time evolution of the isolated benzophenone excited state manifold population as obtained from CAS-SCF non-adiabatic dynamics. D) Potential energy surfaces

over the general coordinate describing the triplet-triplet energy transfer for double insertion (left) and minor groove binding (right) obtained from QM/MM simulations.

Among the many possible photosensitizers benzophenone, despite its limited practical utility for therapeutic purposes, due to its absorption in the UVA range, occupies a paradigmatic and special role. Because of the efficient population of its triplet manifold, benzophenone may trigger many different competitive photosensitization pathways, the most important one being triplet energy transfer to a nearby thymine, as it has been nicely reviewed by Miranda's group [13]. In addition, the inherent photophysics of isolated benzophenone is far from being innocent and trivial, especially due to its three-states quasi-degeneracy involving the first excited singlet and two triplet states [103]. Hence, in this context benzophenone also represents a most suitable example to illustrate the combination of different simulation protocols and level of theories with which computational photobiology may contribute to solve important chemical and biological processes.

The inherent photophysics of benzophenone has been studied by high-level quantum mechanical studies based on complete active space self-consistent field (CAS-SCF) and its second order perturbation theory correction (CAS-PT2), notably by Sergentu *et al.* [103]. The potential energy landscape of benzophenone is dominated by an extended region of quasi-degeneracy between the S_1 state (mainly of $n\pi^*$ character) and the first two triplet state, i.e. T_1 ($n\pi^*$) and T_2 ($\pi\pi^*$). Most notably the quasi-degeneracy region encompasses the S_1 minimum region while the spin-orbit coupling , between S_1 and T_2, also in agreement with the El Sayed rule, is relatively high (~ 20-30 cm^{-1}). Those observations are in agreement with the experimentally observed efficient, almost unitary, intersystem crossing. However, one fundamental question not answered by the previous model concerns the dominant intersystem crossing mechanisms, and in particular if the relaxation proceeds via an intermediate state, i.e. $S_1 \rightarrow T_2 \rightarrow T_1$, or directly, i.e. $S_1 \rightarrow T_1$, with the latter channel being formally excluded by the El Sayed rule but made possible due to the quasi-degeneracy of the involved excited states.

To provide a definitive answer to these questions, CAS-SCF based non-adiabatic molecular dynamics, in the state-hopping framework, and including spin-orbit coupling effects, have been performed for gas-phase benzophenone [104]. Such an approach allows to follow the time evolution of the population of the different electronic states over a statistically relevant number of semi-classical trajectories, hence mimicking the

behavior of a nuclear wavepacket. The non-adiabatic dynamics has confirmed a fast and efficient intersystem crossing, indeed at 600 fs a majority of the trajectories is already in the triplet manifold. Interestingly, while unsurprisingly the population of T_1 is dominating, a persistent population of T_2, reaching up to 10% and behaving like a real spectroscopic state rather than an intermediate can be observed. As far as the kinetic model is concerned, 33% of the trajectory populating the triplet manifold follow the direct $S_1 \rightarrow T_1$ mechanism, while the indirect path is followed by the remaining 67%; hence the two channels have to be considered as competitive. However, the situation is even far more complex and indeed an equilibrium between T_1 and T_2, characterized by constant forward and backward hops between the two states is established. The existence of this equilibrium also justifies the persistent population of T_2 and the absence of its decay.

Coming back to the study of the DNA photosensitization *per se* the first problem one had to face was due to the absence of any experimental structure for the DNA/benzophenone aggregate. In this context, molecular modeling and simulation was fundamental in providing the required answer. Indeed, by using classical molecular dynamics simulation two stable interaction modes between benzophenone and a model polyd(AT) decamer have been identified [105]. While one of the modes was based on the well described minor-groove interaction the second one, styled double-insertion, was observed for the first time. The latter is characterized by the ejection of a full base pair from the DNA double helix and its substitution by the sensitizer. While both modes were stable and persistent in the time scale, hundredths of ns, spanned by the classic molecular dynamics. Subsequently, the binding free energy have been determined [106], by using free energy perturbation (FEP) methodology [107]. The minor groove binding appeared as favored since the corresponding aggregate is stabilized by about 2 Kcal/mol compared to the isolated system.

Since the coupling between benzophenone and the DNA nucleobases differs significantly for the two interaction modes, the triplet-triplet transfer, at the base of photosensitization, was studied for both conformations using a hybrid QM/MM approach, to model the effects of the nucleic acid environment. The photophysical pathway was described taking into account a general coordinate based on the linear interpolation between the equilibrium geometries of the triplet states centered on benzophenone and on the nearest thymine, respectively. The potential energy surfaces of the most relevant excited states have been calculated

at CAS-PT2 and TD-DFT level pointing out an almost barrierless process for the energy transfer from T_1 in case of the double inserted mode, while the minor groove binding presents a considerable barrier of about 0.9 eV [108]. Even though the latter value should be considered as an upper bound due to the use of a linear interpolation coordinate such an energetic penalty should practically impede the photophysical transfer for the minor groove binding mode, which happens to be the thermodynamically favored one. Hence, the question of the efficient triplet transfer experienced by benzophenone remains unanswered. However, as confirmed by the non-adiabatic dynamics the participation of the benzophenone T_2 state should also be taken into account, and indeed a barrierless pathway connecting the triplet centered on benzophenone to the one on thymine exists for this state both in the minor groove and the double inserted mode [108]. Hence, the significant population of the T_2 state should be considered as the key photophysical factor allowing an efficient DNA photosensitization by triplet-triplet energy transfer, a result obtained only by the use of combined multiscale modeling and simulation protocols, including the determination of binding free energy, non-adiabatic dynamics, and high level QM/MM methodologies to take into account the role played by the macromolecular environment.

The DNA environment also play a peculiar role in modulating a minor benzophenone sensitization pathway, namely hydrogen transfer. Indeed, the triplet state of benzophenone induces the homolytic breaking of C-H bonds, a propriety that is also exploited in photocatalysis and polymer science. Once again, the reactive outcomes of the two identified interactions modes should differ considerably: double inserted benzophenone may extract a hydrogen from the thymine methyl group, while the groove bound sensitizer is instead attacking the backbone sugar to ultimately produce strand breaks. However, when considering only a minimal model system composed of benzophenone in its triplet state and the reactive DNA counterpart, i.e. the nucleobase or the sugar respectively, activation energy of less than 10 Kcal/mol are obtained and both reactions are previewed as exergonic [109]. Hence, the question of why such a channel is largely minoritarian in the complex benzophenone sensitization landscape inevitably arises. The answer, once again, comes from a proper multiscale treatment including the analysis of the structure and dynamics of the benzophenone/DNA aggregates. Indeed, when the MD trajectories for both double insertion and groove binding reveal that the benzophenone lies quite distant from the reactive hydrogen, with the distance distribution peaking at around 9 Å. Thus, only a quite marginal

population of distances are compatible with the formation of a prereactive complex. In this sense, one can conclude that DNA actually implements a sort of self-protection, maintaining the benzophenone at sufficient large distances from its reactive moieties to significantly diminish the occurrence of a reaction that, from an electronic point of view, should be fast and favorable [109].

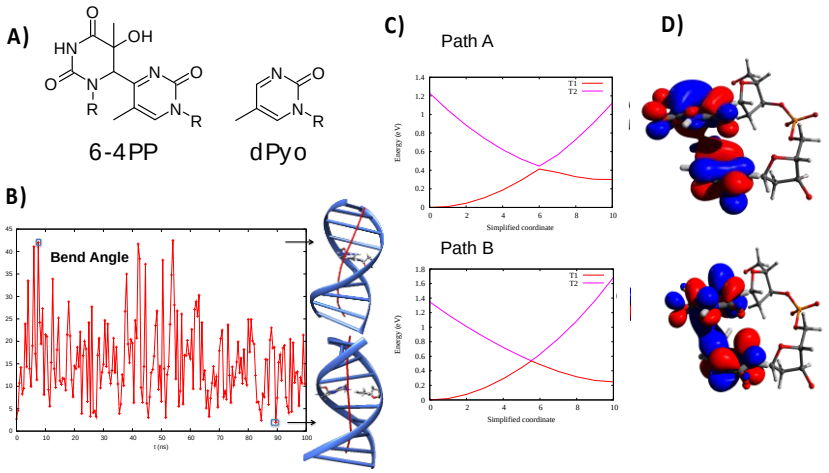

Figure XXXX) A) Molecular formula of the 64-PP and the corresponding chromophoric unit dPyo used to build the artificial nucleobase. B) Time series of the total bending of the dPyo containing DNA oligomer together with two representative snapshots corresponding to the highest and lowest bending, respectively. C) Potential energy surface along the triplet-triplet transfer coordinate for two representative starting conformations, note in Path B the presence of a crossing between the two surfaces. D) Natural transition orbitals describing the unpaired electrons and calculated at the crossing point in Path B showing the delocalization over both unit and the overlap between the functions.

DNA Trojan horses

In the previous subsection we have pointed out how the DNA macromolecular environment can play an efficient protective role. The opposite scenario may however emerge when DNA lesions act as internal photosensitizers. The presence of such "Trojan horses", significantly expanding the possibility of DNA damages formation, has been recognized experimentally by Miranda's group for the very well-known 64-PP. Indeed, the former lesion contains one pyrimidone (Pyo) unit that absorbs light in the UVA range, undergoes a relatively efficient intersystem crossing, and triggers triplet-triplet energy transfer towards nearby thymines [110]. The experimental results, obtained using a modified nucleobase composed of Pyo subunit (dPyo) instead of the full 64-PP lesion, have also been

rationalized via molecular modeling and simulation. In particular by using classical molecular dynamics it has been highlighted that the dPyo artificial nucleobase induces only very minor perturbation in the structure of the DNA double helix, and in particular is not altering the coupling due to the π-stacking arrangement. The triplet-triplet energy transfer has also been studied using the same QM/MM protocol as employed for the benzophenone sensitization, showing that, even though the global driving force appears smaller than for the previous case, the energy transfer is still possible and favorable. Furthermore, in some snapshots the coupling between the two chromophores, i.e. Pyo and Thymine, is found to be extremely high, and gives raise to discontinuities along the potential energy surface that are reminiscent of conical intersections. Such critical points should funnel the transfer phenomena especially in the case of Dexter type triplet transfer, hence contributing to the increase of the efficiency of the full photophysical phenomenon [111].
More recently, the same "Trojan horse" effect has been evidenced for oxidized thymine such as formyl-uracil (ForU). Once again, molecular modeling and simulation have clarified the full photophysical pathways, providing a full mechanistic study of the intersystem crossing events, in particular pointing out its feasibility also due to the absence of significant energy barriers blocking this channel. The triplet-triplet energy transfer has also been characterized and has been found possible and favorable from the point of view of the energy levels alignment. Finally, the effects of the environment, i.e. the DNA double-strand, have been taken into account using a combination of classical molecular dynamics and QM/MM calculations, showing that the perturbation of the DNA structural parameters by ForU is modest or even absent, while the conditions for an efficient intersystem crossing and energy transfer are still present.

DNA Photolesions repair

As previously stated, different repair strategies to remove photolesions exists and are essential to assure viable conditions for both animal and vegetal organisms. Indeed, knocking out the photolesions repair conditions directly results in death or high impairing diseases such as *Xeroderma pigmentosa*. In the following, we present different DNA repair pathways, also focusing on the complex interplay between the structural modifications induced by the lesions and the repair efficiency.

DNA Repair by Photoliases

DNA photolyases are flavoenzymes using sunlight to specifically repair the 64-PP or the CPD DNA damages in many organisms including bacteria, plant, insect, amphibians… Their efficiency relies on a photo-induced electron transfer from the photoexcited reduced flavin adenine dinucleotide ($FADH^-$) buried in the active site and the oxidized damage, flipped-out from the DNA. Many experiments have been performed to elucidate the repair mechanism and the specificity of these proteins. The structures of several photolyases-DNA complexes have been also resolved by X-Ray crystallography [112–114], and have helped to characterize the residues involved in the enzymatic process. Thanks to the photoproperties of the different partners, femtosecond spectroscopy studies have provided catalytic cycles including rate constants for both CPD and 64-PP repair, summarized in Figure XXXX [115]. The CPD repair only involves the reduced FAD and the DNA damage: the electron transfer between them induces the spontaneous and fast (few ps) C-C bonds breaking leading to the recovery of the two adjacent thymines.

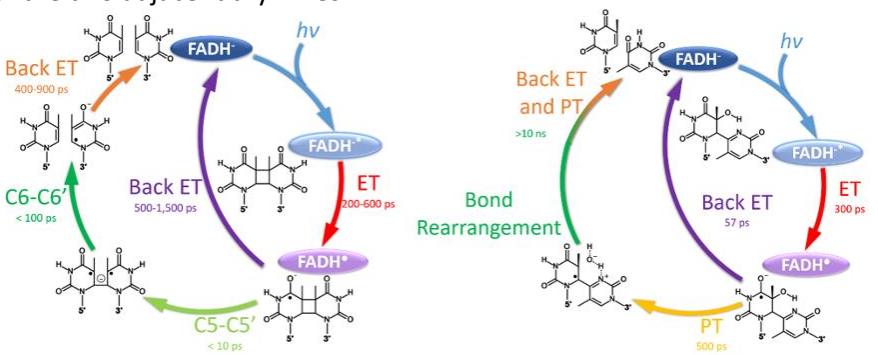

Figure …: CPD photolyase and 6-4 photolyase catalytic cycles. Redraw from (Liu, PCCP, 2015).

The conversion taking place with a high quantum yield of more than 80% [116]. The 6-4 photolyase is way less efficient and has a quantum yield of about 10%, in addition to the photoinduced electron transfer, a proton exchange, involving an histidine in the active site occurs and competes with the futile back electron transfer to FAD. Mutagenesis studies have also illustrated the higher complexity of the 64-PP repair compared to the CPD one: if three mutations are sufficient to convert a 6-4 photolyase into an efficient CPD repair enzyme, the reverse conversion has not been obtained yet, even with 11 mutations in the active site [117].

Classical MD simulations were conducted to understand how photolyases identify a damaged site and flip it into the active site. In CPD photolyase, a classical approach was used to study the flipping-out mechanism with or without the protein [118]. The free energy calculation is based on umbrella sampling with Hamiltonian replica exchange protocol. Both the DNA deformation and the bonding to the protein decrease the free energy penalty required to obtain an extrahelical conformation of the two thymines. The presence of an arginine in the DNA pocket also possibly helps to stabilize the damage in the extrahelical conformation by interacting with the phosphate [119]. Computational approaches also helped to characterize non-covalent interactions in the active site of 6-4 photolyases. The positively-charged amino acids in the DNA pocket play a crucial role in the repair mechanism: a lysine (K246) in the active site of the *Drosophila melanogaster* 6-4 photolyase interacts with the damage and can favor its reduction whereas an arginine (R421) while also interacting with the damage keeps it locked in the active site [120]. These interactions have been further characterized by DFT and hybrid DFT/MM calculations in the homologous active site of *Xenopus laevis* 6-4 photolyase: the guanidino group of the arginine interacts with the negatively charged phosphate groups of the damage and form a cation-π interaction with the 3' nucleobase flanking the 64-PP [121]. However, some 6-4 photolyases, such as PhrB, do not present the homologous lysine or arginine but show an activity dependence to the concentration of divalent cations. The PhrB structure in interaction with DNA has not been resolved yet, but classical MD simulations starting form homologous models have been performed using the crystallographic structure of PhrB alone and the DNA damaged fragment from *Drosophilia melanogaster* photolyase repairing complex. These simulations reveal that two Mg^{2+} enter in the active site and interact with two aspartates, which mutations to asparagine decrease the DNA-repair activity, and with the damage in a similar way as the lysine and the arginine in *Drosophilia melanogaster* photolyase active site [122] (see figure XXXX).

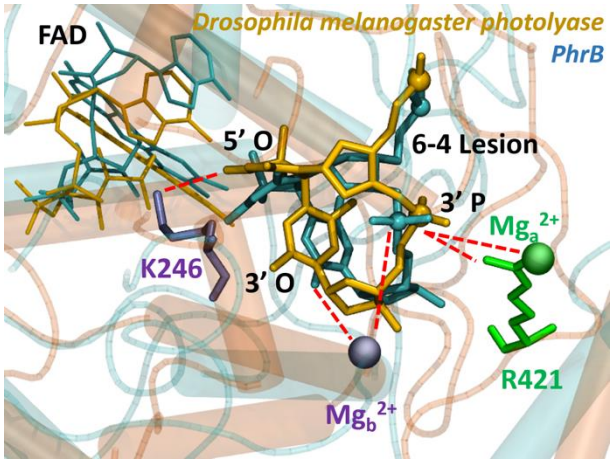

Figure XXX: comparison between the active site of Drosophilia melanogaster 6-4 photolyase (yellow) and PhrB (cyan). K246 and R421 belong to the Dros. mel. Photolyase crystallographic structure (3CVU) and classical simulation have shown that K246 side chain moves toward 3'P. The Mg^{2+} cations belong to the PhrB structure after classical MD simulation. Ask right to (Ma, Febs J, 2019).

When the photodamage is stabilized in the active site, the catalytic repair can start. Despite of the precise rate constant obtained thanks to femtoseconds time-resolved spectroscopy; the chemical mechanisms remains partially unclear. It is widely assumed that the first step consists in an electron transfer from the photoactivated $FADH^-$ to the CPD or 64-PP damages. In more details, the nature, and consequently the rate, of the charge transfer seems structure dependent. Indeed, in the whole photolyase family (including also cryptochrome proteins), the FAD cofactor adopts an unusual U-shape where the isoalloxazine ring and the adenine moiety are more or less stacked. Such a conformation can allow energy and charge exchange between the two π-systems, it is also well established that light absorption produces excitation that are localized on the isoalloxazine moiety. Then, the surrounding environment and the conformation of the DNA damage in its pocket induce different electrostatic field tuning the charge transfer pathway and mechanism. The different rates observed experimentally between the three classes of CPD-Photolyase indicate the coexistence of several electron-transfer mechanisms: a direct tunneling through adenine is dominant in Class I CPD photolyase whereas a two-steps hopping pathway, with a transient negatively-charged adenine, is favored in class II. Class III presents an

intermediate behavior [115]. Using models from class I CPD Photolyase, combinations of classical MDs, excitation energies and electronic coupling calculations support a superexchange mechanism which does not involve the adenine but the methyl group of the isoalloxazine ring [123,124]. Moreover, the wavepacket dynamics describing the electron transfer process, which has been determined solving the time-dependent Schrödinger equation with a finite-difference approach at the DFT/GGA/B3LYP level of theory [125], suggests that adenine polarizes the wave function to drive the transfer toward the CPD lesion damage. The hopping mechanism has also been considered by means of hybrid QM/MM calculations with a high level, multireference description of the excited states (adiabatic diagram correction ADC(2), CASSCF) [126]. The authors conclude to the coexistence of the two mechanisms, in agreement with experiments. The comparison of a set of four CPD photolyases from mesophiles and (hyper)-thermophiles species, based on classical MDs and electron tunneling analysis, shows that the adenine significantly contributes to the electronic coupling of the electron transfer to the damage in the most rigid proteins [127]. At higher temperature, water molecules can compete with adenine to form the best tunneling pathway. A third mechanism has been computationally described, using CASSCF and CASPT2/MM level of theory: a proton-coupled-electron transfer (PCET) involving water molecules bridging the adenine and the 5' thymine of the damage [128]. The resulting strong hydrogen bond enhances the C-C bond cleavage. The crucial role of a strong hydrogen bond to the 5'- damaged thymine has been previously explored by means of QM/MM MDs [119]. The QM zone encompasses the damage and one active site glutamate, and the simulations describe a proton transfer from the glutamate to the lesion, followed by the asynchronous bond cleavage, starting with C5-C5' breaking.

The repair of the 64-PP requires a bond rearrangement which involves the C-O bond cleavage and formation. The activation of the C-O bond is triggered by the proton transfer from an active site histidine and the reduction of the damage, but the exact mechanism remains unclear. Different hypotheses have been proposed based on one or two photon(s) absorption, positively charged or neutral active site histidine, concerted or sequential PCET, oxetane or water intermediates. QM/MM calculations represents a very efficient tool to discriminate the most likely mechanisms by the determination and comparison of energy barriers. In general, only one photoexcitation is considered in the mechanism, but in 2010

Sadeghian *et al* [129] reported a relaxed potential energy surface at DFT/MM level for a mechanism involving an oxetane intermediate and two electron transfers from the FAD which allow to overcome the barrier present in the ground state. Nevertheless, this two excitations hypothesis is not consistent with the experiments. Indeed, due to the natural photon density, the lifetime of an intermediate between two photons absorption should be around 1 ms; spectroscopic signature of such intermediate has not yet been experimentally detected.

Another crucial issue for the elucidation of the repair mechanism is the protonation of the active site histidine, which can be protonated on Nδ, Nε or on both nitrogen atoms. Historically, the positively-charged histidine is preferred, as it should be a better proton donor. However, DFT(B3LYP)/MM calculation of RPE parameters in combination with experiments give no preference to any state, but *pKa* and structural MM studies lead the authors to suggest a neutral histidine, while another active site histidine is supposed to be doubly protonated [130]. High level XMCQDT2-CASSCF calculations of the excitation energies of the active site complex ($FADH^-$, Histidine and DNA damage) also provide argument to the neutral histidine state, as the protonated one would cause a spontaneous PCET which would prevent the repair mechanism [131]. The introduction of the environment (protein, DNA, water and counterions) in a similar CASSCF-CASPT2/MM study slightly counterbalances this conclusion [132]. These calculations showed that the presence of a positively charged histidine decreases the energy of the reduced damage state by 7-20 kcal/mol, but the dead-end PCET is still possible. On the contrary, classical MD [122,133] shows that the double protonated histidine is more consistent with the experimental data concerning both structure and reactivity. Indeed, the RMSD of the histidine and the active site and the His-damage or His-FAD distances (among others) in *Drosophilia melanogaster* photolyase MD are more consistent with the crystallographic data in the presence of positively charged histidine. In PhrB simulation, the behavior of Mg^{2+} cations described earlier is in agreement with mutagenesis studies only if a double protonated histidine is considered. Moreover, the calculation of the repair of the Dewar photoproduct in a model of the 6-4 photolyase active site described at DFT/continuum level gives a lower energy profile in the presence a protonated histidine than a neutral one [134].

Eventually, Faraji and Dreuw performed an exhaustive analysis of the repair mechanism using DFT/MM optimizations, which is summarized in ref [135]. They concluded that a mechanism involving one electron transfer

from $FADH^-$, a proton transfer from the positively charged histidine and the simultaneous intramolecular OH transfer through an oxetane-like intermediate. The QM/MM approach of Dokainish *et al* [136], based on optimization of a large QM zone (982 atoms at DFT –UM062X level after a first optimization of a smaller QM zone -166 atoms), leads to the validation of a quite different mechanism involving the formation of a water molecule during the OH transfer instead of an oxetane-like intermediate and a rate-limiting barrier of 13.4 kcal/mol. When the thymine-thymine damage is replaced by a thymine-cytosine photoproduct, a similar mechanism is obtained with an activation barrier of 20.4 kcal/mol and involving the intermediate formation of a free NH_3, while the energy of the azetidine intermediate is prohibitive (about 60 kcal/mol) [137].

Thus, despite these substantial efforts in computational studies, which assessed the one-photon mechanism with a doubly protonated histidine, the characterization of the 64-PP repair mechanism remains under debate. The different results raise the issue of the definition of the QM zone *vs* QM level, as a higher level of theory supposes less QM atoms. Another issue concerns the dynamical behavior of the photolyase active site. The proton transfer and the bond reorganization are expected to occur at ~500 ps and more than 10 ns respectively, which would let sufficient time to the confined environment to relax with regards to the charge state and the bond arrangement.

Interplay between structural deformations and repair: 64-PP vs. CPD

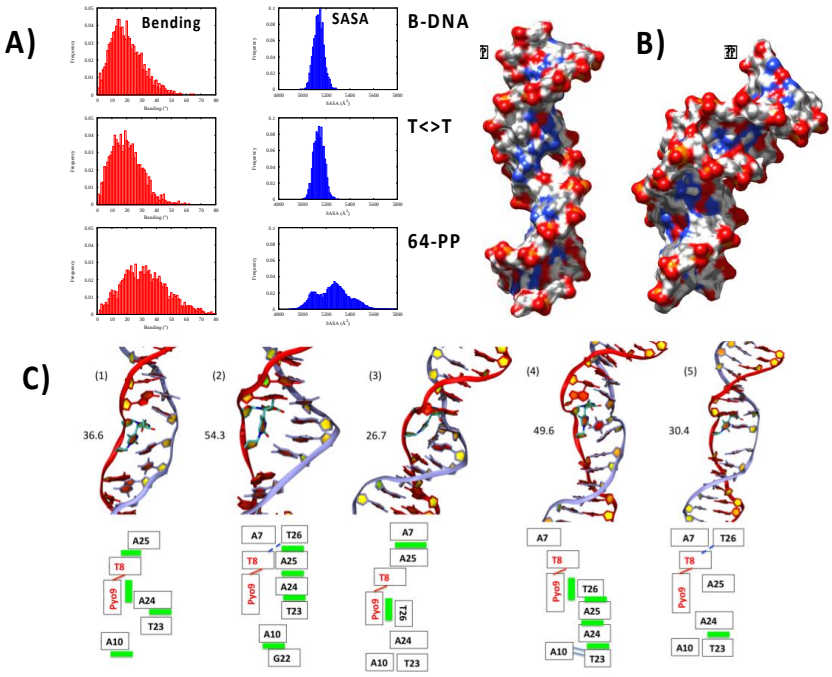

Figure XXX) A) The distribution of the global bending (red) and SASA (blue) for undamaged B-DNA and the corresponding strands containing T<>T and 64-PP lesions respectively. B) Surface representation of two representative snapshots for 64-PP showing the coexistence of straight and bent, as well as compact and hollow structures. C) Cartoon representation of representative conformations observed during the MD simulations together with the schematic representation of the interaction patterns experienced (green boxes represent π-stacking, blue line hydrogens bonds).

In addition to the elucidation of the chemical repair mechanisms, using either static techniques or *ab initio* MD sampling, the complex panorama induced by the structural flexibility of damaged DNA oligonucleotides should be proper dealt with since it can strongly affect the repair rates. Because of the involved large-scale rearrangements, the use of extended sampling via classical MD is compulsory and the case of DNA photolesions, i.e. CPD and 64-PP, is a most paradigmatic example.

Indeed, the repair rate and toxicity of the two photo-lesions are extremely different, and while 64-PP is much easily removed by the NER apparatus is also extremely mutagenic. By using extended classical dynamics exceeding the μs time-scale it has been shown that thymine-thymine CPD (T<>T) are quite rigid and indeed both their global bending and solvent accessible surface are (SASA), the latter being and indicator of the compaction of the

structure, happen to be virtually indistinguishable from the ones typical of undamaged B-DNA strands [57]. On the contrary, 64-PP experiences a veritable polymorphism, and is constantly oscillating between bent and straight forms, as well as between hollow and compact structures. This polymorphisms evidenced by the appearance of different maxima in the distributions of the relevant structural indicators is also accompanied by a major reorganization of the arrangements and π-stacking involving the nucleobases surrounding the lesion also leading to a strong alteration of the original Watson and Crick pairing [57]. The results of the MD simulations have allowed to reconcile contrasting experimental results, that where evidencing bent or straight strands, respectively. More importantly, they provide a rationale for the different repair rate and toxicity, indeed while T<>T, due to the limited structural modifications may easily escape the recognition by the repair machinery, its rigidity induces replication fork blocking, hence strongly limiting its mutagenicity. The much more structurally distorted 64-PP, on the contrary, is readily recognized by the NER machinery and the repair process is efficiently triggered. However, its flexibility and polymorphisms and in particular the disruption of the canonical nucleobases pairing, may be related to a higher rate of replication errors and hence mutations.

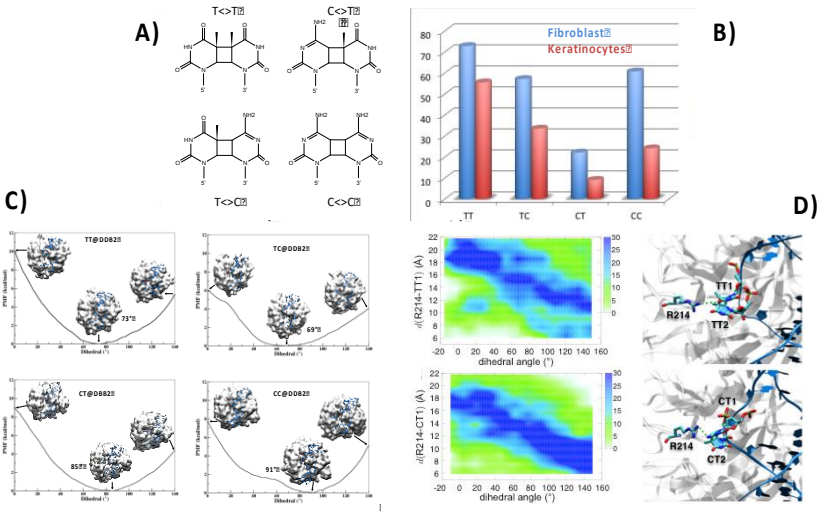

Figure XXX) A) Molecular formula of the four CPD lesions and B) their repair rates in fibroblast and keratinocytes. C) Free energy profile along the dihedral angle defining the spinning of the CPD lesions around the DNA axes obtained for the different CPD lesions showing the more favorable extrusion when the cytosine is in 5' position. D) Analysis of the

distances between the amine (Cytosine) or methyl (Thymine) group and the protonated arginine of DDB2 along the global coordinate.

The rationale behind the more efficient repair of 64-PP, as compared to CPD, has been clearly provided; however other finer effects shuld be proper rationalized. In particular, it has been evidenced that in human skin cells, i.e. fibroblast and keratinocytes, CPD lesions are not repaired with the same efficiency. In particular the presence of a cytosine at the 5' position of the CPD strongly increase the repair rate, hence C<>T and C<>C are removed more efficiently than T<>C and T<>T. While no evident structural differences between the isolated oligonucleotides have been evidenced to justify this behavior, their interaction with the NER recognition factor DDB2 points to subtle, yet significative differences. Indeed, the presence of a 5'-cytosine induces a more pronounced extrusion of the lesion that hence better accommodates in the DDB2 hydrophobic recognition pocket and produces more significant distortion of the protein bound oligomer, hence favoring the subsequent repair steps. The DDB2 lesion extrusion has been characterized by obtaining free energy profiles using the recently developed coupling of extended biased adaptative force (eABF) [138] and metadynamics, styled meta-eABF [139]. The fine molecular reasons for this subtle selectivity have also been traced back to the more favorable interactions developed by the cytosine amine group with the protonated arginine of DDB2. A part for the interest *per se*, such an example is also crucial because it proves how the use of the proper computational methodologies and protocols allows to rationalize not only chemical or biochemical processes but also data issued directly from cellular assays.

Conclusion and perspectives

The fundamental biological role of DNA and the impact of DNA lesions in cell viability or in the development of highly debilitating pathology have clearly justified a large interest by the scientific community and by modeling and simulations. This is also justified by the complexity and the subtle interplay with both the inhomogeneous environment and the diverse signaling pathways happening at cellular level. Hence, the rationalization of DNA lesions, and photolesions inductions in particular, represent a clear scientific challenge that requires proper and finely tailored multiscale approaches, but ultimately allowing to bring answer to fundamental biological questions.

From this standpoint, DNA has been a paradigmatic system for computational biochemistry, with years of intensive efforts by the molecular dynamics community to propose charge-fixed or polarizable force fields that capture the subtle dynamics of the B-DNA backbone at the μs scale. This activity has also taken advantage of high-level quantum mechanics methods to quantify the cooperative non-covalent interactions, hydrogen bonds and π-stacking, that allow DNA to adopt, most often, a B-helix structure. In the same respect the transition between different double helical form (A and Z) and towards non-canonical arrangements, such as guanine-quadruplexes, has also been taken in to account.

The formation of photolesions and the subsequent recognition and repair by dedicated enzymes has profited from intensive research efforts by several pioneer groups that have used advanced computational methods to determine potential or free energy surfaces related to mechanical (such as damage extrusion) of electronic events (electron or charge transfer). These protocols have shown an increasing degree of complexity tackling both the isolated model systems and the macromolecular environments. Hybrid QM/MM simulations have particularly proven their capability to complement experimental data, notably by clarifying by the exploration of the complex energy landscapes determining the occurrence of complex chemical reactivity such as the rationalization of various transport phenomena based on charge, electron, or hydrogen (proton) transfer. The complementarity and the interaction between simulation and experiments has been built in the last two decades and while leading to significant progress in the field, it has also allowed the clear emergence of molecular computational biology approaches. Notably, the accuracy in the description of transfer phenomena, has also allowed the treatment of DNA based materials with potential applications in the field of organic and molecular optoelectronics.

Despite the impressive success of the simulations of DNA lesions and the answer that have been brought to the community, one main limitation of computational approaches is somehow due to the consideration of model systems presenting regular sequences, such as poly(dG), poly(dG-dC), poly(dA) and poly(dA-dT), hence limiting the understanding of subtle structural andx electronic sequence-dependent effects. Undoubtedly, such an approach is due to the relatively high computational cost necessary for the study of different sequences whose complexity grew combinatorially, and by the related difficulty in the analysis of the complex data obtained.

As in many scientific fields the interplay between the development of more efficient computational protocols and the machinery of artificial intelligence (IA) will certainly provide consistent breakthroughs in the nearby future, both in term of increased computational power and analytical rationalization of complex and multivaried series of data.
Another aspect that will be crucial in the following years and that should be strongly improved will be the analysis of the role of complex non-canonical environment on the production and outcome of DNA lesions. This will include the study of the role of DNA lesions happening in the nucleosomal environment, i.e. with the oligomer wrapped around histones proteins. A part from the size of the systems, important complexity will arise by the interplay with intrinsically disordered structures, the histone tails, and by the opening of novel, and the tuning of existent photochemical pathways, such as tautomerization [140] or protein-DNA cross-link formation [141], induced by the strongly inhomogeneous and highly charged nucleosomal environment. Finally, a fascinating, yet at the moment rather unexplored field, will be the exploration of the role of DNA lesions, and photolesions, in the control of gene expression. Recent experimental [142] and computational [143] results, indeed point to an important role of DNA lesions in modulating the epigenetic regulation.

Despite the limitations that should be considered carefully, it is evident that the computational study of DNA lesions also constitutes a paradigmatic example in which by using proper multiscale approaches, and by dealing with both the electronic and structural effects on an equal footing the answer to relevant biological questions becomes possible. This in turn bring an unprecedented and complementary point of view able to achieve an atomic and molecular scale resolution of crucial phenomena, and in the long term will also lead to the definition of protective strategies or to the rational development of novel DNA-interacting photodrugs.
In other words, we strongly believe that the study of DNA has strongly contributed to the affirmation of molecular computational photobiology as a fundamental approach to complement the more classical experimental determination in chemistry and molecular biology. I has also contributed to settle down some of the principle to which a reliable computational photobiology should adhere, namely the strong interplay with experimental sciences, and the fully multiscale approach aiming at providing an unified description of different temporal and spatial scales.

In this respect, we believe that, also by profiting from the impressive methodological development, the time from computational photobiology to come on and shine is definitively just in front of us.

References

1. J. E. Klaunig, L. M. Kamendulis, and B. A. Hocevar, Toxicol. Pathol. **38**, 96 (2010).
2. R. P. Sinha and D.-P. Häder, Photochem. Photobiol. Sci. **1**, 225 (2002).
3. T. B. Kryston, A. B. Georgiev, P. Pissis, and A. G. Georgakilas, Mutat. Res. - Fundam. Mol. Mech. Mutagen. **711**, 193 (2011).
4. T. B. Salmon, Nucleic Acids Res. **32**, 3712 (2004).
5. R. B. Hamanaka and N. S. Chandel, Trends Biochem. Sci. **35**, 505 (2010).
6. J. Cadet, J.-L. Ravanat, G. R. Martinez, M. H. G. Medeiros, and P. di Mascio, Photochem. Photobiol. **82**, 1219 (2006).
7. S. Miyamoto and P. Di Mascio, Subcell. Biochem. **77**, 3 (2014).
8. T. Finkel, J. Cell Biol. **194**, 7 (2011).
9. J. Cadet and J. R. Wagner, Cold Spring Harb. Perspect. Biol. **5**, a012559 (2013).
10. E. Factors, *Skin Stress Response Pathways* (Springer, 2016).
11. M. Valko, D. Leibfritz, J. Moncol, M. T. D. Cronin, M. Mazur, and J. Telser, Int. J. Biochem. Cell Biol. **39**, 1 (2006).
12. B. Epe, Photochem. Photobiol. Sci. **11**, 98 (2012).
13. M. C. Cuquerella, V. Lhiaubet-Vallet, J. Cadet, and M. A. Miranda, Acc. Chem. Res. **45**, 1558 (2012).
14. T. C. Evans and N. M. Nichols, Annu. Rev. Biochem. **57**, 1 (2008).
15. X. X. Huang, F. Bernerd, and G. M. Halliday, Am. J. Pathol. **174**, 1534 (2009).
16. A. Ziegler, D. J. Leffell, S. Kunala, H. W. Sharma, M. Gailani, J. A. Simon, A. J. Halperin, H. P. Baden, P. E. Shapiro, and A. E. Bale, Proc. Natl. Acad. Sci. U. S. A. **90**, 4216 (1993).
17. R. Drouin and J. P. Therrien, Photochem. Photobiol. **66**, 719 (1997).
18. D. E. Brash, J. A. Rudolph, J. A. Simon, A. Lin, G. J. McKenna, H. P. Baden, A. J. Halperin, and J. Pontén, Proc. Natl. Acad. Sci. U. S. A. **88**, 10124 (1991).
19. J. S. Taylor, Acc. Chem. Res. **27**, 76 (1994).
20. N. J. Curtin, Nat. Rev. Cancer **12**, 801 (2012).
21. E. Sage and L. Harrison, Mutat. Res. - Fundam. Mol. Mech. Mutagen. **711**, 123 (2011).
22. M. Goldstein and M. B. Kastan, Annu. Rev. Med. **66**, 129 (2015).

23. A. J. Breugom, M. Swets, J. F. Bosset, L. Collette, A. Sainato, L. Cionini, R. Glynne-Jones, N. Counsell, E. Bastiaannet, C. B. M. van den Broek, G. J. Liefers, H. Putter, and C. J. H. Van de Velde, Lancet Oncol. **16**, 200 (2015).
24. S. M. Crafton and R. Salani, Clin. Ther. **38**, 449 (2016).
25. F. M. J. Schabel, M. W. Trader, W. R. J. Laster, T. H. Corbett, and D. P. J. Griswold, Cancer Treat. Rep. **63**, 1459 (1979).
26. D. E. Lehane, R. N. Bryan, B. Horowitz, L. Desantos, G. Ehni, M. A. Zubler, R. Moiel, L. Rudolph, A. Aldama-Leubbert, D. Mahoney, and R. Harper, Cancer Drug Deliv. **1**, 69 (1983).
27. M. J. Peckham, A. Horwich, and W. F. Hendry, Br. J. Cancer **52**, 7 (1985).
28. J. P. Cerón-Carrasco, D. Jacquemin, and E. Cauët, Phys. Chem. Chem. Phys. **14**, 12457 (2012).
29. B. W. Henderson and T. J. Dougherty, Photochem. Photobiol. **55**, 145 (1992).
30. E. Zenkevich, E. Sagun, V. Knyukshto, A. Shulga, A. Mironov, O. Efremova, R. Bonnett, S. P. Songca, and M. Kassem, J. Photochem. Photobiol. B Biol. **33**, 171 (1996).
31. E. Koshi, A. Mohan, S. Rajesh, and K. Philip, J. Indian Soc. Periodontol. **15**, 323 (2011).
32. T. Dai, Y. Y. Huang, and M. R. Hamblin, Photodiagnosis Photodyn. Ther. **6**, 170 (2009).
33. R. R. Allison and K. Moghissi, Photodiagnosis Photodyn. Ther. **10**, 331 (2013).
34. F. Reessing and W. Szymanski, Curr. Med. Chem. **24**, 4905 (2017).
35. S. H. C. Askes, G. U. Reddy, R. Wyrwa, S. Bonnet, and A. Schiller, J. Am. Chem. Soc. **139**, 15292 (2017).
36. S. Bonnet, B. Limburg, J. D. Meeldijk, R. J. M. K. Gebbink, and J. A. Killian, J. Am. Chem. Soc. **133**, 252 (2011).
37. Y. Kuang, H. Sun, J. C. Blain, and X. Peng, Chem. - A Eur. J. **18**, 12609 (2012).
38. S. T. Howell, L. A. Cardwell, and S. R. Feldman, Curr. Dermatol. Rep. **7**, 43 (2018).
39. L. A. Schneider, R. Hinrichs, and K. Scharffetter-Kochanek, Clin. Dermatol. **26**, 464 (2008).
40. S. M. Yoon, Y. G. Park, E. S. Park, and C. Y. Choi, Med. Lasers **6**, 5 (2017).
41. J. M. Ortiz-Salvador and A. Pérez-Ferriols, in (Springer, Cham, 2017), pp. 279–286.
42. T. S. Colin Theng and E. S.-T. Tan, in (Springer, Cham, 2018), pp. 235–

252.
43. S. L. H. Higgins and K. J. Brewer, Angew. Chemie - Int. Ed. **51**, 11420 (2012).
44. J. Cadet, T. Delatour, T. Douki, D. Gasparutto, J.-P. Pouget, J.-L. Ravanat, and S. Sauvaigo, Mutat. Res. Mol. Mech. Mutagen. **424**, 9 (1999).
45. J. Cadet, E. Sage, and T. Douki, Mut. Res. Fund. Mol. Mec. Mut. **571**, 3 (2005).
46. S. P. Scott and T. K. Pandita, J. Cell. Biochem. **99**, 1463 (2006).
47. A. Mehta and J. E. Haber, Cold Spring Harb. Perspect. Biol. **6**, a016428 (2014).
48. P. J. McKinnon and K. W. Caldecott, Annu. Rev. Genomics Hum. Genet. **8**, 37 (2007).
49. W. J. Cannan and D. S. Pederson, J. Cell. Physiol. **231**, 3 (2016).
50. E. Dumont and A. Monari, Front. Chem. **3**, 43 (2015).
51. E. Dumont, R. Grüber, E. Bignon, C. Morell, Y. Moreau, A. Monari, and J. L. Ravanat, Nucleic Acids Res. **44**, 56 (2016).
52. R. D. Hazel, K. Tian, and C. de Los Santos, Biochemistry **47**, 11909 (2008).
53. C. A. Gelfand, G. E. Plum, A. P. Grollman, F. Johnson, and K. J. Breslauer, Biochemistry **37**, 7321 (1998).
54. L. Ayadi, C. Coulombeau, and R. Lavery, J Biomol Struct Dyn **17**, 645 (2000).
55. C. D. Mol, T. Izumi, S. Mitra, and J. A. Talner, Nature **403**, 451 (2000).
56. H. L. Lo, S. Nakajima, L. Ma, B. Walter, A. Yasui, D. Ethell, and L. B. Owen, BMC Cancer **5**, 135 (2005).
57. F. Dehez, H. Gattuso, E. Bignon, C. Morell, E. Dumont, and A. Monari, Nucleic Acids Res. **45**, 3654 (2017).
58. C. J. Park, J. H. Lee, and B. S. Choi, Photochem. Photobiol. **83**, 187 (2007).
59. E. Sage, R. Drouin, and M. Rouabhia, in *From DNA Photolesions to Mutat. Ski. Cancer Cell Death* (The Royal Society of Chemistry, 2005), pp. 15–31.
60. H. Ikehata and T. Ono, J. Radiat. Res. **52**, 115 (2011).
61. A. Frances-Monerris, J. Segarra-Marti, M. Merchan, and D. Roca-Sanjuan, Theor. Chem. Acc. **135**, 31 (2016).
62. C. Clauson, O. D. Scharer, and L. Niedernhofer, Cold Spring Harb. Perspect. Biol. **5**, a012732 (2013).
63. F. A. Derheimer, J. K. Hicks, M. T. Paulsen, C. E. Canman, and M. Ljungman, Mol Pharmacol **75**, 599 (2009).

64. E. Bignon, T. Dršata, C. Morell, F. Lankaš, and E. Dumont, Nucleic Acids Res. **45**, 2188 (2017).
65. N. Y. Tretyakova, A. Groehler, and S. Ji, Acc. Chem. Res. **48**, 1631 (2015).
66. E. Bignon, C.-H. Chan, C. Morell, A. Monari, J.-L. Ravanat, and E. Dumont, Chem. - A Eur. J. **23**, (2017).
67. S. Silerme, L. Bobyk, M. Taverna-Porro, C. Cuier, C. Saint-Pierre, and J. L. Ravanat, Chem. Res. Toxicol. **27**, 1011 (2014).
68. A. G. Georgakilas, P. O'Neill, and R. D. Stewart, Radiat. Res. **180**, 100 (2013).
69. A. G. Georgakilas, P. V Bennett, and B. M. Sutherland, Nucleic Acids Res. **30**, 2800 (2002).
70. A. G. Georgakilas, P. V Bennett, D. M. Wilson, and B. M. Sutherland, Nucleic Acids Res. **32**, 5609 (2004).
71. H. Gattuso, E. Durand, E. Bignon, C. Morell, A. G. Georgakilas, E. Dumont, C. Chipot, F. Dehez, and A. Monari, J. Phys. Chem. Lett. **7**, 3760 (2016).
72. E. Bignon, H. Gattuso, C. Morell, F. Dehez, A. G. Georgakilas, A. Monari, and E. Dumont, Nucleic Acids Res. **44**, 8588 (2016).
73. H. E. Krokan and M. Bjørås, Cold Spring Harb. Perspect. Biol. **5**, 1 (2013).
74. A. B. Robertson, A. Klungland, T. Rognes, and I. Leiros, Cell. Mol. Life Sci. **66**, 981 (2009).
75. S. S. Wallace, DNA Repair (Amst). **19**, 14 (2014).
76. A. K. Mantha, B. Sarkar, and G. Tell, Mitochondrion **16**, 38 (2014).
77. S. S. David, V. L. O'Shea, and S. Kundu, Nature **447**, 941 (2007).
78. A. Sancar and M. S. Tang, Photochem. Photobiol. **57**, 905 (1993).
79. J. Hu, O. Adebali, S. Adar, and A. Sancar, Proc. Natl. Acad. Sci. 201706522 (2017).
80. O. D. Schärer, Cold Spring Harb. Perspect. Biol. **5**, a012609 (2013).
81. J. A. Marteijn, H. Lans, W. Vermeulen, and J. H. J. Hoeijmakers, Nat. Rev. Mol. Cell Biol. **15**, 465 (2014).
82. E. Mladenov, S. Magin, A. Soni, and G. Iliakis, Front. Oncol. **3**, 113 (2013).
83. E. Mladenov, S. Magin, A. Soni, and G. Iliakis, Semin. Cancer Biol. **37**–**38**, 51 (2016).
84. E. Bignon, H. Gattuso, C. Morell, F. Dehez, A. G. Georgakilas, A. Monari, and E. Dumont, Nucleic Acids Res. **44**, 8588 (2016).
85. C. Han, A. K. Srivastava, T. Cui, Q. E. Wang, and A. A. Wani, Carcinogenesis **37**, 129 (2015).

86. B. D. Price and A. D. D'Andrea, Cell **152**, 1344 (2013).
87. C. Fonseca Guerra, F. M. Bickelhaupt, J. G. Snijders, and E. J. Baerends, J. Am. Chem. Soc. **122**, 4117 (2000).
88. C. Fonseca Guerra, F. M. Bickelhaupt, J. G. Snijders, and E. J. Baerends, Chem. - A Eur. J. **5**, 3581 (1999).
89. F. Zaccaria, G. Paragi, and C. Fonseca Guerra, Phys. Chem. Chem. Phys. **18**, 20895 (2016).
90. J. Szolomájer, G. Paragi, G. Batta, C. F. Guerra, F. M. Bickelhaupt, Z. Kele, P. Pádár, Z. Kupihár, and L. Kovács, New J. Chem. **35**, 476 (2011).
91. P. D. Dans, I. Ivani, A. Hospital, G. Portella, C. González, and M. Orozco, Nucleic Acids Res. **45**, 4217 (2017).
92. A. Perez, I. Marchán, D. Svozil, J. Sponer, T. E. Cheatham, C. A. Laughton, and M. Orozco, Biophys. J. **92**, 3817 (2007).
93. R. Galindo-Murillo, J. C. Robertson, M. Zgarbová, J. Šponer, M. Otyepka, P. Jurečka, and T. E. Cheatham, J. Chem. Theory Comput. **12**, 4114 (2016).
94. M. Zgarbová, J. Šponer, M. Otyepka, T. E. Cheatham, R. Galindo-Murillo, and P. Jurečka, J. Chem. Theory Comput. **11**, 5723 (2015).
95. M. Nygaard, T. Terkelsen, A. Vidas Olsen, V. Sora, J. Salamanca Viloria, F. Rizza, S. Bergstrand-Poulsen, M. Di Marco, M. Vistesen, M. Tiberti, M. Lambrughi, M. Jäättelä, T. Kallunki, and E. Papaleo, Front. Mol. Biosci. **3**, 78 (2016).
96. M. Lambrughi, L. De Gioia, F. L. Gervasio, K. Lindorff-Larsen, R. Nussinov, C. Urani, M. Bruschi, and E. Papaleo, Nucleic Acids Res. **44**, 9096 (2016).
97. L. Etheve, J. Martin, and R. Lavery, Nucleic Acids Res. **44**, 9990 (2016).
98. S. Faraji and A. Dreuw, Annu. Rev. Phys. Chem. **65**, 275 (2014).
99. S. A. P. Lenz and S. D. Wetmore, J. Phys. Chem. B **121**, 11096 (2017).
100. J. Sebera, Y. Hattori, D. Sato, D. Reha, R. Nencka, T. Kohno, C. Kojima, Y. Tanaka, and V. Sychrovsky, Nucleic Acids Res. **45**, 5231 (2017).
101. J. Aranda, M. Roca, V. López-Canut, and I. Tuñón, J. Phys. Chem. B **114**, 8467 (2010).
102. J. Aranda, F. Attana, and I. Tuñón, ACS Catal. **7**, 1728 (2017).
103. D.-C. Sergentu, R. Maurice, R. W. A. Havenith, R. Broer, and D. Roca-Sanjuán, Phys. Chem. Chem. Phys. **16**, 25393 (2014).
104. M. Marazzi, S. Mai, D. Roca-Sanjuán, M. G. Delcey, R. Lindh, L. González, and A. Monari, J. Phys. Chem. Lett. **7**, 622 (2016).
105. E. Dumont and A. Monari, J. Phys. Chem. Lett. **4**, 4119 (2013).
106. H. Gattuso, E. Dumont, C. Chipot, A. Monari, and F. Dehez, Phys. Chem. Chem. Phys. **18**, 33180 (2016).

107. C. Chipot and A. Pohorille, *Free Energy Calculations: Theory and Applications in Chemistry and Biology* (Springer, 2007).
108. E. Dumont, M. Wibowo, D. Roca-Sanjuán, M. Garavelli, X. Assfeld, and A. Monari, J. Phys. Chem. Lett. **6**, 576 (2015).
109. M. Marazzi, M. Wibowo, H. Gattuso, E. Dumont, D. Roca-Sanjuán, and A. Monari, Phys. Chem. Chem. Phys. **18**, 7829 (2016).
110. V. Vendrell-Criado, G. M. Rodríguez-Muñiz, M. C. Cuquerella, V. Lhiaubet-Vallet, and M. A. Miranda, Angew. Chemie - Int. Ed. **52**, 6476 (2013).
111. E. Bignon, H. Gattuso, C. Morell, E. Dumont, and A. Monari, Chem. - A Eur. J. **21**, 11509 (2015).
112. A. Mees, T. Klar, P. Gnau, U. Hennecke, A. P. M. Eker, T. Carell, and L. O. Essen, Science (80-.). **306**, 1789 (2004).
113. M. J. Maul, T. R. M. Barends, A. F. Glas, M. J. Cryle, T. Domratcheva, S. Schneider, I. Schlichting, and T. Carell, Angew. Chemie - Int. Ed. **47**, 10076 (2008).
114. S. Kiontke, Y. Geisselbrecht, R. Pokorny, T. Carell, A. Batschauer, and L. O. Essen, EMBO J. **30**, 4437 (2011).
115. M. Zhang, L. Wang, and D. Zhong, Photochem. Photobiol. **93**, 78 (2017).
116. Z. Liu, L. Wang, and D. Zhong, Phys. Chem. Chem. Phys. **17**, 11933 (2015).
117. D. Yamada, H. M. Dokainish, T. Iwata, J. Yamamoto, T. Ishikawa, T. Todo, S. Iwai, E. D. Getzoff, A. Kitao, and H. Kandori, Biochemistry **55**, 4173 (2016).
118. A. Knips and M. Zacharias, Sci. Rep. **7**, 41324 (2017).
119. F. Masson, T. Laino, U. Rothlisberger, and J. Hutter, ChemPhysChem **10**, 400 (2009).
120. K. A. Jepsen and I. A. Solov'yov, Eur. Phys. J. D **71**, 155 (2017).
121. Y. Terai, R. Sato, T. Yumiba, R. Harada, K. Shimizu, T. Toga, T. Ishikawa-Fujiwara, T. Todo, S. Iwai, Y. Shigeta, and J. Yamamoto, Nucleic Acids Res. **46**, 6761 (2018).
122. H. Ma, D. Holub, N. Gillet, G. Kaeser, K. Thoulass, M. Elstner, N. Krauß, and T. Lamparter, FEBS J. **286**, 1765 (2019).
123. J. Antony, D. M. Medvedev, and A. A. Stuchebrukhov, J. Am. Chem. Soc. **122**, 1057 (2000).
124. T. R. Prytkova, D. N. Beratan, and S. S. Skourtis, Proc. Natl. Acad. Sci. U. S. A. **104**, 802 (2007).
125. A. Acocella, G. A. Jones, and F. Zerbetto, J. Phys. Chem. B **114**, 4101 (2010).

126. W. Lee, G. Kodali, R. J. Stanley, and S. Matsika, Chem. - A Eur. J. **22**, 11371 (2016).
127. B. J. G. Rousseau, S. Shafei, A. Migliore, R. J. Stanley, and D. N. Beratan, J. Am. Chem. Soc. **140**, 2853 (2018).
128. H. Wang, X. Chen, and W. Fang, Phys. Chem. Chem. Phys. **16**, 25432 (2014).
129. K. Sadeghian, M. Bocola, T. Merz, and M. Schütz, J. Am. Chem. Soc. **132**, 16285 (2010).
130. K. Condic-Jurkic, A. S. Smith, H. Zipse, and D. M. Smith, J. Chem. Theory Comput. **8**, 1078 (2012).
131. T. Domratcheva, J. Am. Chem. Soc. **133**, 18172 (2011).
132. A. R. Moughal Shahi and T. Domratcheva, J. Chem. Theory Comput. **9**, 4644 (2013).
133. H. M. Dokainish and A. Kitao, ACS Catal. **6**, 5500 (2016).
134. Y. J. Ai, R. Z. Liao, S. L. Chen, W. J. Hua, W. H. Fang, and Y. Luo, J. Phys. Chem. B **115**, 10976 (2011).
135. S. Faraji and A. Dreuw, Photochem. Photobiol. **93**, 37 (2017).
136. H. M. Dokainish, D. Yamada, T. Iwata, H. Kandori, and A. Kitao, ACS Catal. **7**, 4835 (2017).
137. H. M. Dokainish and A. Kitao, J. Phys. Chem. B **122**, 8537 (2018).
138. T. Zhao, H. Fu, T. Lelièvre, X. Shao, C. Chipot, and W. Cai, J. Chem. Theory Comput. **13**, 1566 (2017).
139. H. Fu, H. Zhang, H. Chen, X. Shao, C. Chipot, and W. Cai, J. Phys. Chem. Lett. **9**, 4738 (2018).
140. A. Francés-Monerris, H. Gattuso, D. Roca-Sanjuán, I. Tuñón, M. Marazzi, E. Dumont, and A. Monari, Chem. Sci. **9**, 7902 (2018).
141. C.-H. Chan, A. Monari, J.-L. Ravanat, and E. Dumont, Phys. Chem. Chem. Phys. **21**, 23418 (2019).
142. A. M. Fleming, J. Zhu, S. A. Howpay Manage, and C. J. Burrows, J. Am. Chem. Soc. **141**, 11036 (2019).
143. Hognon, Gebus, Barone, and Monari, Antioxidants **8**, 337 (2019).